

1- to 2-nm-wide nanogaps fabricated with single-walled carbon nanotube shadow masks

E. P. De Poortere^{a),b)} and H. L. Stormer^{a)}

Department of Physics, Columbia University, New York, New York 10027

L. M. Huang,^{a)} S. J. Wind,^{a)} and S. O'Brien^{a)}

Department of Applied Physics and Applied Mathematics, Columbia University, New York, New York 10027

M. Huang^{a)} and J. Hone^{a)}

Department of Mechanical Engineering, Columbia University, New York, New York 10027

(Received 31 May 2006; accepted 2 October 2006; published 4 December 2006)

The authors present a method for producing nanometer-scale gaps, based on metal evaporation through a suspended single-walled carbon nanotube acting as a shadow mask. 83% of the nanogap devices display current-voltage dependencies characteristic of direct electron tunneling. Fits to the current-voltage data yield gap widths in the 0.8–2.3 nm range for these devices, dimensions that are well suited for single-molecule transport measurements. © 2006 American Vacuum Society. [DOI: 10.1116/1.2375081]

As the gate lengths of silicon field-effect transistors continue their steady descent into the sub-100 nm range, electronic devices based on novel elements such as nanowires or single organic molecules are increasingly being explored as alternatives to conventional semiconductor technology. Single-molecule transistors, in particular, have proven difficult to evaluate, as such devices appear to be highly sensitive to the manner in which the molecule is contacted.¹ Experiments based on electromigrated metal leads² or mechanical break junctions,³ for example, have yielded some insights into the workings of few-molecule junctions, though their behavior remains far from understood. In particular, the use of electromigration to generate nanoscale gaps is somewhat problematic, as this method is known to give rise to fairly disordered gaps containing metal islands or clusters,⁴ which make conductance data difficult to interpret.⁵ This issue imposes serious limits on interpreting current-voltage data obtained with such devices: single-molecule transport experiments ideally require a large number of clean and similar metal junctions.

In this article, we present a nanogap fabrication technique based on a single-walled nanotube (SWNT) shadow mask, in which the dimension of the junction is controlled solely by the diameter of the nanotube and by its distance from the substrate during metal deposition. This scheme has been applied in the past with thicker multiwalled carbon nanotubes or SWNT bundles^{6,7} to create gaps wider than ~20 nm. Here we rely on a mechanical transfer technique developed recently by Huang *et al.*⁸ to place long, quasiparallel, individual SWNT's onto a surface patterned with an electron-beam resist film. In this way, a given nanotube is suspended over ten parallel "trenches" in the patterned resist; after

metal deposition and lift-off, the method thus gives rise to ten nanoscale gaps *defined by the same nanotube*. We measure the current-voltage characteristics of 79 wires produced with this method and deduce from tunneling data that 66 of these have widths in the 0.8–2.3 nm range. Only 2 out of 79 wires are shorted.

The metal and substrate materials selected for this study are Pt and ZrO₂, respectively. Our choice is inspired by reports that the growth of Pt films over clean cubic ZrO₂(100) crystals is two dimensional,^{9,10} in contrast to the typical grainlike growth of noble metals on oxides.¹¹ This layer-by-layer film growth allows us, in principle, to work with metal films much thinner than those used traditionally for this type of device, which are typically up to tens of nanometer thick. Using ultrathin metal films allows us in turn to reduce the thickness of the resist film, and therefore to reduce the nanometer-scale broadening of features caused by the finite size of the metal source during Pt evaporation. Very importantly, thin Pt films also result in shallower junctions whose structure and contents could be observed by scanning probes.¹²

The devices are made from *n*-doped Si substrates, coated with 3.7- or 9.1-nm-thick ZrO₂ films formed by atomic layer deposition (ALD). We first use standard electron-beam lithography to pattern long, narrow trenches in a resist bilayer [Fig. 1(a)], developed for 1 min in a 1:3 H₂O:isopropanol cosolvent at ~4 °C with ultrasonic agitation. The lower resist layer is a MMA/8.5/MAA EL1.5 copolymer spun cast at 4000 rpm for 45 s, and the upper layer 495 K PMMA A1 spun at 3000 rpm for 60 s (both resists were purchased from Microchen Corp.), and baked at temperatures in the 180–200 °C range. This coating results in a total resist thickness of about 35 nm. On a separate Si "carrier" chip, long SWNT's are grown by chemical vapor deposition, using ethanol as carbon feedstock and a 1-nm-thick Co film as catalyst, according to a technique detailed in Refs. 8 and 13.

^{a)}Also at Center for Electron Transport in Molecular Nanostructures, Columbia University, New York, NY 10027.

^{b)}Electronic mail: etienne@phys.columbia.edu

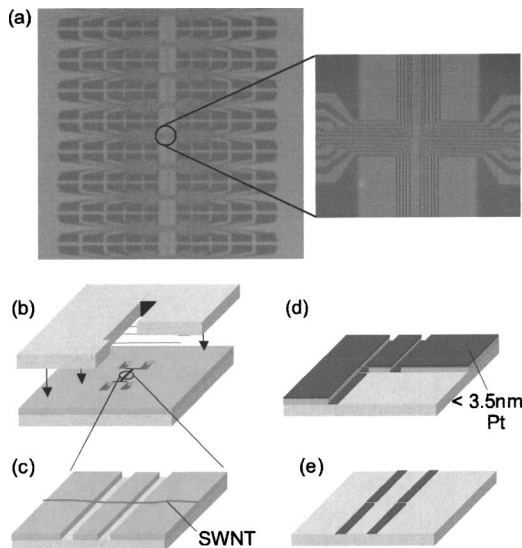


FIG. 1. Sample fabrication steps. (a) Optical micrograph of resist pattern after electron-beam exposure and development (light green: substrate; darker color: unexposed resist). Ten 100-nm-wide trenches (highlighted for clarity) run down the central section of the pattern and are connected at $90\ \mu\text{m}$ intervals to the contact pads. (b) Single-walled nanotubes are transferred to the resist-coated sample by pressing the carrier chip onto the resist-patterned sample. SWNT sections that were suspended on the carrier chip adhere preferentially to the resist and break off from the rest of the original nanotube. For clarity, only two trenches are shown, and at a larger scale. (c) Detail of central area of the sample: SWNT now rests over lithographically defined trenches in the 35-nm-thick copolymer/PMMA resist. (d) Up to 3.5 nm Pt are deposited over the sample, forming a wire and a nanometer-scale gap opening underneath the overhanging nanotube. (e) Excess metal is removed after lift-off.

These wafers contain $100\ \mu\text{m} \times 1\ \text{mm}$ window slits over which typically four to ten carbon nanotubes rest suspended after growth.

We then transfer the nanotubes from their carrier chip onto the sample containing the patterned resist by bringing the two samples into contact [Fig. 1(b)] using an optical mask aligner.⁸ The suspended part of the nanotubes on the carrier chip adheres to the resist on the Si/ZrO₂ sample, and remains on it when the two samples are separated, breaking away from the other nanotube sections [Fig. 1(c)]. The slit on the carrier sample can be easily aligned with the resist trenches under the microscope, so that the nanotubes, once transferred on the resist, are now suspended above the trenches. This method allows us currently to transfer one to four nanotubes from a carrier chip, though this number can probably be increased by minimizing particulate density on the samples or by reducing the total contact area between carrier and resist samples.¹⁴ Since at present we have no precise control over the location of the nanotubes grown across the slit, we designed a redundant, 1-mm-long, wire pattern that essentially spans the whole length of the slit on the SWNT carrier chip [Fig. 1(a)]. Contact pads are placed every $\sim 90\ \mu\text{m}$ along the length of the wires, so as to ensure that at most one nanogap is found between two successive contact pads on average.

Following the nanotube transfer, we deposit $\sim 3.5\ \text{nm}$ Pt onto the patterned sample by electron-beam evaporation, us-

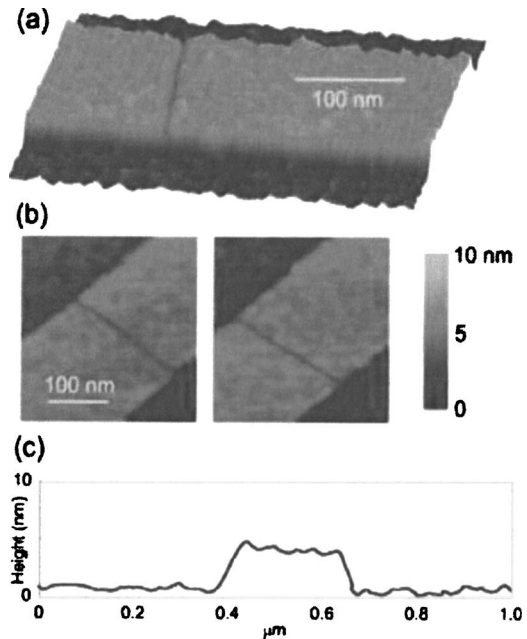


FIG. 2. [(a) and (b)] AFM scans of device, showing a gap in the Pt metal line formed by the SWNT shadow mask. (b) Scans of two different wires with gaps, produced using the *same* nanotube. (c) Transversal line scan of a Pt wire, showing that the roughness of the Pt surface and of the ZrO₂ substrate are similar (the rms roughness for both is $\sim 0.35\ \text{nm}$).

ing a rate of $0.2\text{--}0.4\ \text{\AA}/\text{s}$. Prior to lift-off, we image a central section of the sample in a scanning electron microscope in order to locate the transferred nanotubes and their positions with respect to alignment marks. Imaging the samples and finding nanogaps *after* lift-off is much more difficult in our case, because of the poor contrast offered by the ultrathin films we use. We also note that the design of the evaporation chamber and of the metal source are critical for nanometer-scale gap fabrication, since wide sources or short evaporation distances can taper the edges of the deposited metal by a few nanometers. Our Pt source is about 5 mm wide, and the source-to-sample distance 75 cm in our process. Given these dimensions, the nanotube shadow width may be reduced by up to $0.2\ \text{nm}$,⁶ much less than the diameter of the smallest SWNT. After metal deposition, the sample is placed in boiling acetone for 2 h and dipped in an ultrasound bath for 30 s–1 min in the same solvent. These steps ensure the removal of both resist and nanotubes, as well as that of the metal in the unpatterned areas.

A potential problem with this technique is that of nanotube sagging, which can cause the tubes to adhere to the oxide surface exposed at the bottom of the trenches, and ultimately prevent these tubes from lifting off properly after metal evaporation. We designed the trenches to be 35 nm deep and 40–200 nm wide, and were able to lift off easily all nanotubes transferred on these samples, indicating that this is not an issue for our samples.

Figure 2 shows atomic force microscope (AFM) scans of some of our devices. A narrow, continuous groove cuts across the Pt wire, a result of the shadow evaporation of the metal around the suspended nanotube. The gap width is dif-

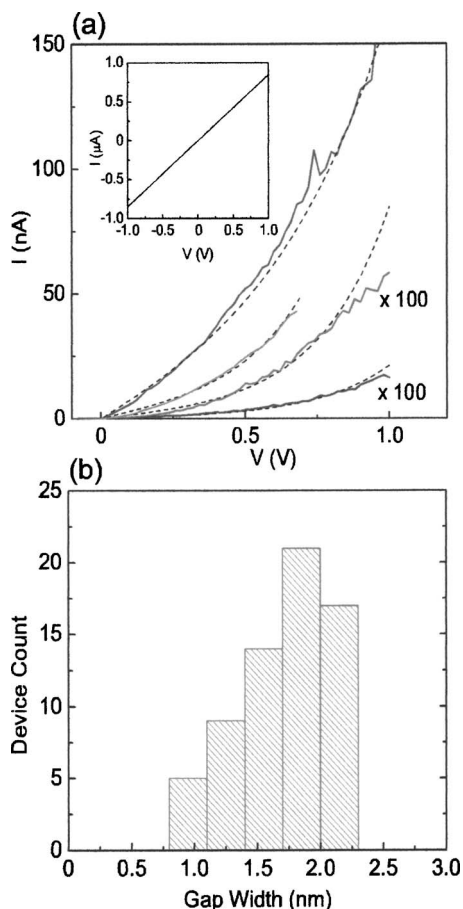


FIG. 3. (a) Current-voltage data for four nanogaps, showing nonlinear dependence characteristic of direct tunneling. The devices measured here were obtained from four parallel wires “cut” by the same nanotube. Dashed curves: calculated fits to the data using the Simmons model (Ref. 17). Calculated gap widths are, from top to bottom, 1.3, 1.8, and 2 nm for the last two curves. Inset: I - V data for a 3.5-nm-thick Pt wire ($40\text{ nm} \times 90\text{ }\mu\text{m}$) with no nanogap. (b) Histogram of gap widths obtained from I - V tunneling data for 66 different wires. Most of the widths fall within the 1–2 nm range.

difficult to determine precisely from AFM scans because of the finite size of the scanning tip, but can be inferred from measurements of the tunneling current across the gap, as detailed below, and shown to be smaller than ~ 2.5 nm. Several gaps are produced in this fashion from each nanotube, suspended across a sequence of parallel trenches. The resulting gaps are shown for two Pt wires in Fig. 2(b).

The line scan of the metal line [Fig. 2(c)] shows that the apparent roughness of the Pt film is comparable to that of the underlying oxide, indicating that the film, in spite of its small thickness, can form a continuous layer on ZrO_2 . Film continuity is also confirmed by conductance measurements, discussed below.

We study electrical transport through these wires and gaps in air and at room temperature. Wire thicknesses are about 3.5 nm for three of our devices, and about 2.5 nm for the fourth one, and the uncut wires we measured are $\sim 90\text{ }\mu\text{m}$ long and 40–100 nm wide. 3.5-nm-thick wires have a total resistance of 0.6–1.2 M Ω , i.e., $\sim 700\text{ }\Omega/\text{sq}$ [see inset of Fig. 3(a)].¹⁵ We note that these resistances, although in the

megaohm range, are small relative to typical resistances of metal-molecule-metal bridges¹⁶ and can be further reduced by appropriate design. We then study a total of 79 wires interrupted by nanogaps and show data for four of these in Fig. 3(a). 66 of these wires show electron transport characteristic of direct tunneling, while the I - V traces are linear—and hence the gaps shorted—in only 2 out of the 79 wires. The remaining 11 gaps carry a current smaller than about 10 pA at 2 V bias. In contrast, most wires produced during the same process, but not shadowed by SWNT’s, do not show tunneling I - V ’s.

We analyze the I - V ’s of all 66 “tunneling” wires by fitting our data to Simmons’ model,¹⁷ taking into account the influence of the image charge within the gap. In this model, gap width, barrier height, and tunneling area are fitting parameters.¹⁸ Although the model uses three different fitting parameters, the global curvature of the calculated tunneling I - V is highly sensitive to the choice of gap width only. The resulting uncertainty on the gap width, based on this fitting, is about ± 0.2 nm. Data and calculated curves for some of the devices are plotted in Fig. 3(a). We obtain gap widths ranging from 0.8 to 2.3 ± 0.2 nm, with a median gap width smaller than 2 nm.¹⁹ A histogram of these data is shown in Fig. 3(b): we note that these widths are consistent with the measured diameter range of the nanotubes used in our process, 0.8–1.8 nm, obtained from Raman scattering data.¹³

In summary, we have developed a technique for creating thin nanoscale metal junctions, whose widths are controlled by the diameter of a SWNT shadow mask. The yield of gaps in the tunneling range (0.8–2.3 nm here) is larger than 80%, and less than 3% of the devices are shorted, indicating that the gaps are likely free of metal clusters. In addition, this technique helps to avoid e-beam resist contamination issues at the metal gap, a potential problem with direct electron-beam lithography. These devices are thus well suited for single-molecule transport measurements, which require excellent control over gap fabrication at the nanometer scale. Finally, the 2.5–3.5 nm metal thickness used in our process opens up the possibility of imaging with scanning probes single-molecule devices based on these metal films.

The authors thank Evgeni Gusev for the ALD growth, and Philip Kim for access to the AFM. They also thank Henry Huang for helpful discussions about the nanotube transfer technique. This work was supported by the Nanoscale Science and Engineering Initiative of the National Science Foundation under NSF Award No. CHE-0117752, by the NSF Grant No. PHY-0103552, by the New York State Office of Science, Technology, and Academic Research (NYSTAR), and by a grant from the W. M. Keck Foundation.

¹H. Basch, R. Cohen, and M. A. Ratner, *Nano Lett.* **5**, 1668 (2005).

²J. Park *et al.*, *Nature (London)* **417**, 722 (2002).

³J. Reichert, R. Ochs, D. Beckmann, H. B. Weber, M. Mayor, and H. von Löhneysen, *Phys. Rev. Lett.* **88**, 176804 (2002).

⁴A. de Picciotto, J. E. Klare, C. Nuckolls, K. Baldwin, A. Erbe, and R. L. Willett, *Nanotechnology* **16**, 3110 (2005).

⁵R. Sordan, K. Balasubramanian, M. Burghard, and K. Kern, *Appl. Phys. Lett.* **87**, 013106 (2005).

- ⁶J. Lefebvre, M. Radosavljević, and A. T. Johnson, *Appl. Phys. Lett.* **76**, 3828 (2000).
- ⁷J. Chung, K. H. Lee, and J. Lee, *Nano Lett.* **3**, 1029 (2003).
- ⁸X. M. H. Huang, R. Caldwell, L. Huang, S. C. Jun, M. Huang, M. Y. Sfeir, S. P. O'Brien, and J. Hone, *Nano Lett.* **5**, 1515 (2005).
- ⁹S. Roberts and R. J. Gorte, *J. Phys. Chem.* **95**, 5600 (1991).
- ¹⁰P. A. Dilara and J. M. Vohs, *J. Phys. Chem.* **99**, 17259 (1995).
- ¹¹C. T. Campbell, *Surf. Sci. Rep.* **27**, 1 (1997).
- ¹²Recently, we were able to extend the SWNT template method to Si/SiO₂ substrates, using ~1.5 nm Ni as an adhesion layer and ~3 nm Pt as wire material.
- ¹³L. M. Huang, B. White, M. Y. Sfeir, M. Y. Huang, H. X. Huang, S. Wind, J. Hone, and S. O'Brien, *J. Phys. Chem. B* **110**, 11103 (2006).
- ¹⁴Rayleigh scattering measurements [see M. Y. Sfeir, F. Wang, L. M. Huang, C.-C. Chuang, J. Hone, S. P. O'Brien, T. F. Heinz, and L. E. Brus, *Science* **306**, 1540 (2004)] allow us to check that most of the suspended nanotubes on the carrier chip are unbundled, though some do form pairs or triplets.
- ¹⁵The 2.5-nm-thick wires were approximately six times more resistive than the 3.5-nm-thick ones, although the former were measured after an acryl strip cleaning step, which likely oxidizes part of the Pt.
- ¹⁶A. Salomon, D. Cahen, S. Lindsay, J. Tomfohr, V. B. Engelkes, and C. D. Frisbie, *Adv. Mater. (Weinheim, Ger.)* **15**, 1881 (2003).
- ¹⁷J. G. Simmons, *J. Appl. Phys.* **34**, 1793 (1963).
- ¹⁸In principle, electrons tunnel through both air and the underlying ZrO₂ substrate, though additional simulations show that the oxide carries a much smaller direct tunneling current than air. In practice, we simplify the model by assuming that only one "effective" material, with a relative permittivity equal to 1, separates the electrodes.
- ¹⁹The barrier height parameters that best fit our data vary between 4 and 6 eV. This energy variation probably results from the sensitivity of the metal work function to adsorbed gases.